Available online at www.sciencedirect.com

ScienceDirect

Procedia Manufacturing 51 (2020) 842–847

Procedia MANUFACTURING

www.elsevier.com/locate/procedia

30th International Conference on Flexible Automation and Intelligent Manufacturing (FAIM2020)
15-18 June 2020, Athens, Greece.

Electron beam weld modelling of ferritic steel: effect of prior-austenite grain size on transformation kinetics

A.N. Vasileiou[a]*, C.J.Hamelin[b,c], M.C. Smith[a], J.A. Francis[a], Y.L. Sun[a,d], T. F. Flint[a], Q. Xiong [a], V. Akrivos[a]

[a]*The University of Mancheseter,M13 9PL, Manchester, UK*
[b]*Australian Nuclear Science and Technology Organisation, NSW 2234, Lucas Heights , Australia*
[c]*EDF Energy, Barnett Way, Barnwood, Gloucester GL4 3RS, UK*
[d]*Cranfield University, Cranfield, MK43 0AL, UK*

* Corresponding author. Tel.: +44 (0) 161 275 1912. *E-mail address:* anastasia.vasileiou@manchester.ac.uk

Abstract

Ferritic steels experience solid-state phase transformation (SSPT), which causes volumetric changes due to differences in the atomic packing density of different phases in the steel. The importance of the prior austenite grain size (PAGS) as an input physical variable is assessed, for adequately modelling the anisothermal SSPT during welding of ferritic steels. The knowledge of the PAGS value pre-requires a thorough microstructural study of each particular weld, information that might be difficult to acquire. A relationship between hardness, PAGS and phase fractions is proposed to be used to feed in weld models. The case of a single-pass, autogenous, reduced-pressure electron beam weld is used for this study. The adequacy of the finite-element weld model in predicting the micro-constituents, the hardness and the residual stress is demonstrated via comparing the predicted results of the thermo-metallurgical and stress analyses with the set of corresponding experimental data. This work aims at providing a better understanding of the impact of PAGS on transformation kinetics and best practice guidelines for modelling, using an extensively validated electron beam weld model as baseline.

Keywords: Electron beam welding; phase transformation; microstructure; prior-au9stenite grain size; residual stress; modelling

1. Introduction

Low-alloy steels that undergo solid-state phase transformations (SSPT) are widely being used in power plants [1]. The joining techniques currently used for manufacturing and repair of components are mainly arc welding techniques, varying from traditional manual metal arc and gas-tungsten arc to more innovative narrow-groove arc welding. In recent years, electron beam (EB) welding has been the focus of research activities, as it offers the prospect of high production rates with subsequent economic advantages. Extensive understanding of electron beam welds' performance in-service is essential, prior to their application in a new construction. Residual stress has been identified as a parameter that affects the through-life integrity of components. Experimental techniques like the incremental deep-hole drilling and the neutron diffraction have proved successful in measuring the residual stress field [2–5]. Recent studies present a comparison between single-pass EB welding and narrow-groove arc welding [6–8].

Weld modelling has become a tool for the development of welding and repair techniques. Validated weld models can predict the thermal transients [9], the residual stress [10,11] and deformation fields [12] and the resulting microstructure [13],

10.1016/j.promfg.2020.10.118

which subsequently enables understanding and managing through-life structural performance of welds.

Modelling of low-alloy steels has the complexity of having to take into account solid state phase transformation (SSPT) [10,13–19]. SSPT causes volumetric changes due to differences in the atomic packing density of the different phases in the steel. As demonstrated in [14] especially for EB welds that are single-pass and autogenous, SSPT has a significant effect on the stress distribution in the fusion zone (FZ) and the heat-affected zone (HAZ). Anisothermal SSPT during welding of ferritic steels has been experimentally approached for SA508 Grade 3 Class 1 steel [16,20–22].

The present work aims at identifying a correlation between prior-austenite grain size (PAGS) and phase-fractions (martensite, ferrite, perlite) as well as PAGS and hardness on a SA508 Grade 3 Class 1 EB weld, through a thoroughly validated weld model.

Nomenclature

SSPT	solid-state phase transformation
PAGS	prior austenite grain size
RPEB	reduced-pressure electron beam
TCs	thermocouples
ND	neutron diffraction
CM	contour method
EDM	electro-discharge machining
FZ	fusion zone
HAZ	heat-affected zone
SEM	scanning electron microscope
UoM	The University of Manchester
NDE	non-destructive evaluation
NNUMAN	New Nuclear MANufacturing

2. Methodology

The prior austenite grain size (PAGS) is an input parameter required to model the anisothermal SSPT during welding. The knowledge of the PAGS value pre-requires a thorough microstructural study of each particular weld, information that might be difficult to acquire. Subsequently, it is essential to (i) assess its impact on the results; that would make any characterisation effort valuable and (ii) consider alternative options for estimating the PAGS value, for instance using hardness as a surrogate. Both these goals are explicitly presented in this work.

The case of a single-pass, autogenous, reduced-pressure electron beam weld is used for this study. The adequacy of the finite-element weld model in predicting the hardness and the residual stress is demonstrated via comparing the predicted results of the thermo-metallurgical and stress analyses with the set of corresponding experimental data.

The weld was instrumented with thermocouples, samples were extracted for metallography and hardness mapping, and residual stresses were measured using two independent techniques: neutron diffraction and the contour method. The experiment and the measurements were designed to assist weld modelling, providing all the data required for validation at every stage.

Both a two-dimensional (2D) and a three-dimensional (3D) model were created. The models followed a sequentially coupled approach, that included (a) model creation, (b) heat source validation, (c) thermo-metallurgical analysis, and (d) mechanical-metallurgical analysis.

The 2D model was used for the sensitivity analysis on the PAGS. From these analyses, the PAGS number that approached the measured hardness (HV) value was chosen as the ‘best model’. The 3D analysis run for the input parameters of the ‘best model’ and its results were compared to the measured residual stresses.

3. Experiments

3.1. Electron beam welding

Two Reduced-Pressure Electron Beam (RPEB) welds were manufactured at The Welding Institute (TWI), Cambridge, UK following the NNUMAN manufacturing protocol [7,23,24]. The welds were made of the SA508 Gr.3 Cl.1 nuclear reactor pressure vessel steel (Table 1), and the dimensions of the final welds were 300 x 200 x 30 mm. The welding was performed in the 2G-position (Fig. 1), in TWI’s vacuum chamber. The welding parameters were a voltage of 150 kV, current of 90 mA, pre-heating temperature of 104^{o}C, 200 mm/min travel speed and 3x10^{-2} mbar chamber pressure.

Table 1. Composition of SA508 Grade 3 Class 1 in weight percent (wt%).

C	Si	Mn	Cr	Co	Ni
0.16	0.27	1.43	0.23	0.004	0.77
Mo	S	P	CEV	Fe	
0.52	0.002	0.005	0.605	Bal.	

The second weld was produced was to prove repeatability of the experimental parameters and the measurements, but also to produce enough material for additional residual stress measurements. Each plate were instrumented with eight (8) thermocouples (TCs): four on the front surface (Fig. 1) and four on the back surface, placed symmetrically, at 7mm and 15mm from the weld centreline, on a plane at mid-length.

The non-destructive evaluation (NDE) that was performed using radiography showed that both welds were accepted according to the ASME IX:2013 acceptance criteria.

Fig. 1. One of the two SA508 Gr.3 Cl.1, 30mm thick RPEB welds.

3.2. Residual stress measurements

Residual stresses were measured using two independent techniques: the non-destructive neutron diffraction (ND) and the destructive contour method (CM). An initial neutron diffraction residual stress measurements experiment was performed using the Engin-X beam line at the ISIS Neutron and Muon Source in the U.K. A repeat measurement was performed at the Kowari instrument, at ANSTO in Australia. The details of the neutron diffraction experiment are described in [14] and [23]. The details of the contour method experiment are described in [25]. The plane of interest is the plane at mid-length and the line at mid-thickness, representative of steady state conditions.

3.3. Metallography and hardness

Slices were extracted from the weld and were metallographically prepared and examined. A macrograph (Fig. 2) was produced. Scanning electron microscopy (SEM) was used to qualitatively assess the microstructure of the weld. The fusion zone (FZ) and the heat-affected zone (HAZ) were identified to contain a mix of bainitic and martensitic structures. The parent material is a tempered bainitic structure. Image J and literature conventions [26] were used to measure PAGS.

A hardness map was produced (Fig. 2) using a DurascanTM Vickers microhardness machine, with 0.5kg load and 20s dwell period. The hardness value variation is in agreement with the SEM microscopy findings.

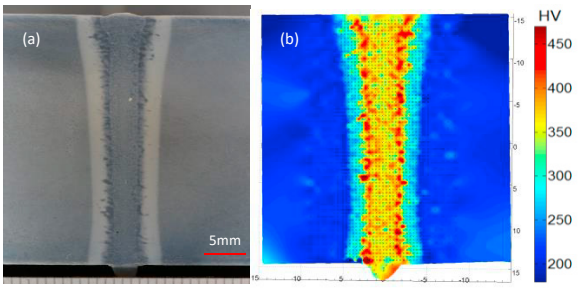

Fig. 2. (a) Macrograph of the RPEB weld [23]; (b) Hardness map [6].

4. Weld modelling

4.1. Cases Examined

A two-dimensional (2D) model was developed for the PAGS sensitivity study and the ten cases presented in Table 2 were considered. Sequentially coupled thermo-metallurgical analyses were run and the results included the predicted hardness and the predicted micro-constituents (martensite/bainite).

The results were plotted in a single graph. Using the measured hardness value, a PAGS value was deduced and was subsequently compared to the experimentally measured one.

For the case that was identified as the best one, a three-dimensional (3D) model was developed, in order to assess its adequacy in predicting residual stresses.

Table 2. Cases modelled in 2D with varying grain size as input parameters

Case #	Grain size (μm)
(A)	10
(B)	20
(C)	50
(D)	100
(E)	200
(F)	500
(G)	1000
(H)	2000
(I)	5000

4.2. Modelling Approach

4.2.1. Thermal model

The main finite element analysis (FEA) software used for the weld modelling was Abaqus. A second FE software, FEAT-WMT (Weld Modelling Tool) [27] was used for heat-source modelling. Using the Abaqus mesh, FEAT-WMT inputs were adjusted to calibrate the heat source against thermocouple data and a macrograph (Fig. 2) [14]. Input parameters were the welding conditions (section 3.1), the heat source parameters, the material properties (specific heat, conductivity, latent heat, Solidus, Liquidus) and thermal boundary conditions (convection, radiation).

A conical heat source was employed to model the EB, based on a 2D Gaussian distribution in the plane of the metal surface and a linear variation down into the material. The coefficients a, c_1, c_2, that were used to describe the radii in the lateral direction, the axial direction ahead of the torch and after the torch, were set to 0.97mm, 0.8mm and 0.8mm respectively. Coefficient b_c, describing the distance vertically downwards from the torch centre where the conical distribution falls to zero, was set to 30mm. An efficiency of 57% was selected via an iterative process to match the "far-field" thermocouple data, a value that is consistent with literature [28]. The heat source was imported to Abaqus through DFLUX and UEXTERNALDB user routines.

The mesh of the 2D thermal model comprised 3100 quadratic, quadrilateral elements DC2D8, whereas the mesh of the 3D model comprised 25000 DC3D20 elements. The material parameters were obtained from [13]. The mesh was dense at the area of the fusion zone and the heat-affected zone and was coarser towards the edges of the specimen.

4.2.2. Metallurgical model

For the metallurgical model, the modelling scheme proposed by Hamelin et al. [13], which included the use of a SSPT subroutine developed at ANSTO, was used. The SSPT subroutine (UVARM, USFLD, UAMP) assigns different field variables for the different phases or microconstituents that are present at any location in the model. Austenitisation is modelled using the Leblond and Devaux model [29], austenite grain growth is captured via the Ikawa et al. approach, the decomposition of austenite is upon cooling is modelled using the Li model [30] and the Koistinen-Marburger model is used for the martensitic transformation. The ASTM grain size (PAGS) is an input parameter for the Li model, in particular for

the equation that predicts the time required for a volume fraction of a given phase to transform at a certain temperature.

4.2.3. Mechanical model

The mechanical analysis reads the thermal field from the thermal analysis and is coupled with the metallurgical analysis. A UEXPAN subroutine is used, to assign various coefficients of thermal expansion, depending on the microstructure. UEXPAN reads the field variable for phase composition and applies the necessary thermal and transformation strains. The hardening behaviour of SA508 Gr3 Cl1 is typically modelled using a pure kinematic hardening law. The mechanical properties used are described in [13] and include the temperature-dependent constitutive response of SA508 Gr.3 Cl.1 steel, phase-dependent yield stress for the austenitic and relevant ferritic phases (ferrite, bainite, martensite), and work-hardening behaviour for the austenitic phase and the relevant ferritic phases.

5. Results and Discussion

Quantification of the effect of PAGS on the predicted phase fractions is presented in Fig. 3 and Fig. 4.

Observing the resulting martensite percentage (Fig. 3) and the resulting bainite percentage (Fig. 4) in the FZ and the HAZ for cases (A) to (I), in the form of contour plots, it quickly becomes obvious that for the thermal cycles that a 30mm thick SA508 Gr3 Cl1 experiences during electron beam welding, the resulting microstructures is generally martensitic – bainitic.

For small PAGS values (10-20μm) 100% bainite is predicted in the FZ and the HAZ. As the PAGS increases to 50–200μm, the microstructure in the FZ becomes a mixture of martensite and bainite at 40-60% fractions whereas the HAZ remains bainitic. Higher PAGS values (500μm to 5mm) result in a fully martensitic microstructure. In all cases, two bands of 50% bainite-martensite are present, which are possibly due to numerical discontinuities at the FZ-HAZ and the HAZ-base metal interfaces.

Fig. 5 is a combinatorial graph; The horizontal, logarithmic axis is the PAGS value, the green line with its values on the left vertical axis is the predicted martensite fraction at a point in the weld centre line, at mid-thickness, as indicated by the arrow in the sub-figure. The purple line, with its values on the right vertical axis, corresponds to the predicted hardness at the same location. The experimentally measured hardness value (Fig. 2) is ~330HV. Following the orange indicators on the graph, if the hardness in the fusion zone is known, then using the present study can offer an approximation of the PAGS value in the FZ. Using Fig. 5 and a measured hardness value, the PAGS value suggested by the graph is 34μm. From SEM microscopy (section 3.3), the measured PAGS in the FZ is 26.4 μm, however the value in the weld centreline is, surprisingly, 34μm. In both cases, the value estimated by Fig. 5 was very close to the actual, measured PAGS. Subsequently, Fig. 5 could be used as a reference when the PAGS value is difficult to measure.

Furthermore, based on the same graph, an estimation of the martensite fraction can be made. Knowing in advance the

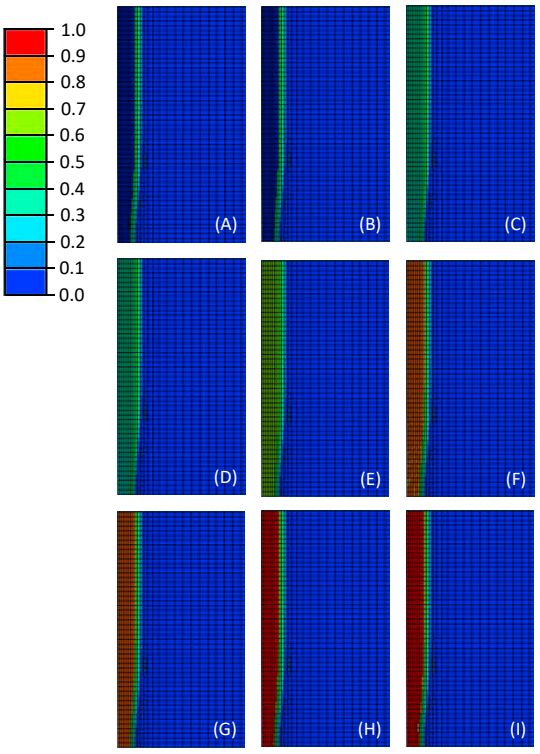

Fig. 3. Martensite predictions for PAGS equal to (a) 10 microns, (b) 20 microns, (c) 50 microns, (d) 100 microns, (e) 200 microns, (f) 500 microns, (g) 1 mm, (h) 2 mm, (i) 5 mm.

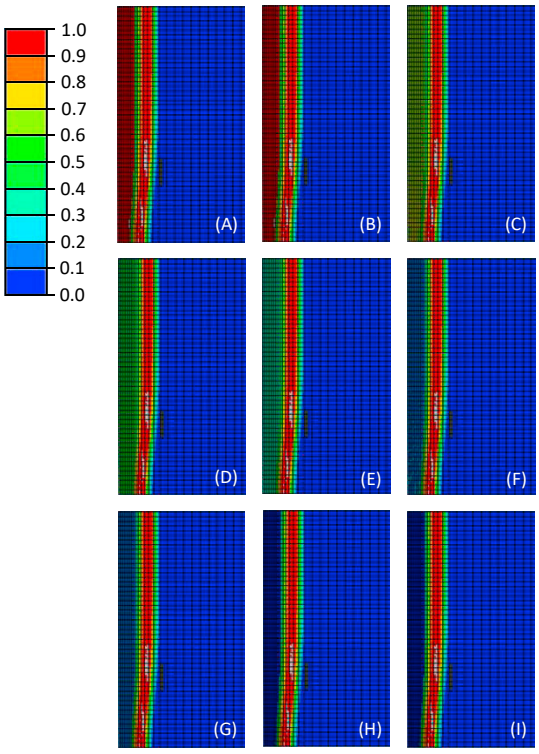

Fig. 4. Bainite predictions for PAGS equal to (a) 10 microns, (b) 20 microns, (c) 50 microns, (d) 100 microns, (e) 200 microns, (f) 500 microns, (g) 1 mm, (h) 2 mm, (i) 5 mm.

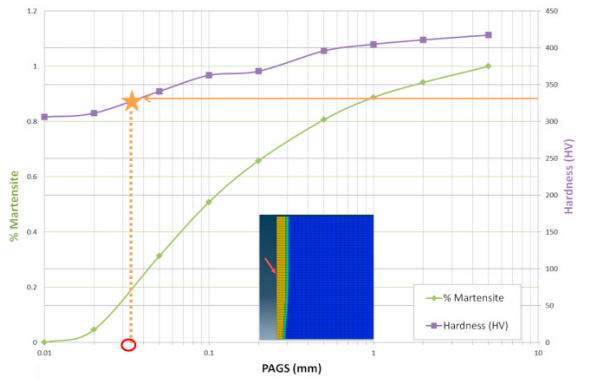

Fig. 5. Predicted martensite fraction (%) and predicted hardness (HV) as a function of PAGS.

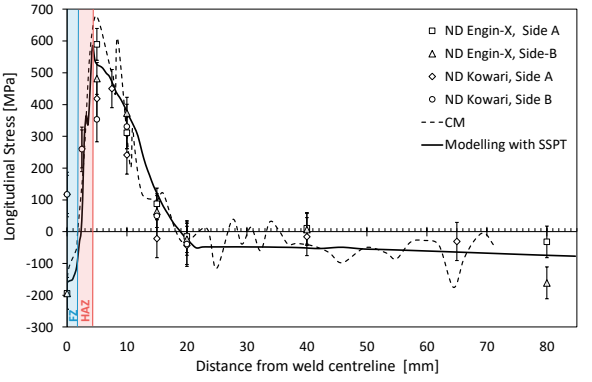

Fig. 7. Residual stress line plots: numerical analysis results versus ND and CM experimental measurements.

expected phase fraction could be very useful in cases where a simplified model is to be used; rather than explicitly modelling SSPT, sometimes it is preferable to make an estimation of the resulting microstructure in the FZ and the HAZ, assign the relevant material properties and proceed with the finite element analysis. Such a simplification is typical for other ferritic steel welds, that result in a e.g. pure martensitic microstructure, but is not typical for SA508 Gr3 Cl1, that usually results in a mixture of microconstituents. In this respect, Fig. 5 could be a useful tool.

Using the PAGS value from the previous study, a thermal-metallurgical-mechanical analysis was performed in 3D. The scope was to showcase whether using a realistic value for PAGS results in a realistic stress field. Fig. 6 shows how the temperature field and a microconstituent develop in 3D, while the electron beam is still running. In Fig. 6a, the grey region in

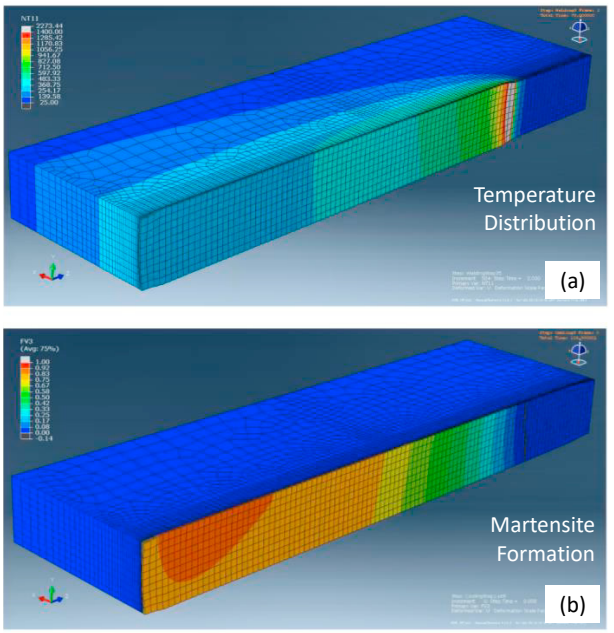

Fig. 6. Weld modelling indicative results shown on the half model: (a) temperature distribution and (b) martensite formation.

the mesh corresponds to the metal that is molten at this particular time frame.

The results of the 3D analysis are plotted in Fig. 7 in the form of a line plot, extracted from the model at mid-thickness. In the same plot, experimental stress measurements, taken from 12.5-15mm below the upper surface of the weld using neutron diffraction and contour method, are shown. The ND measurements along a horizontal line were symmetrical with respect to the weld centre line, plotted here accordingly as "Side A" and "Side B". The residual stresses are ~-200MPs compressive in the FZ and rapidly begin to develop to highly tensile (600-700MPs) stresses just outside the HAZ. Only 20mm away from the weld centerline, the stresses drop near-zero levels.

The agreement between numerical prediction and experimental measurement is very good, given the challenging stress gradient and the inherent measurement technique's uncertainties [31].

6. Conclusions

The case of a thoroughly characterized, 30mm, single-pass electron beam weld from the low-alloy steel SA508 Grade 3 Class 1 was used to demonstrate and quantify the effect of the prior-austenite grain size (PAGS) value on the resulting microstructure through weld modelling.

The knowledge of PAGS, with certain levels of accuracy, proved significant. However, measuring the PAGS is expensive as it requires extracting a metallography slice from the weldment and performing optical and SEM microscopy.

The present work suggests the use of hardness values as a surrogate, to deduce the PAGS and then use this value as an input to a SSPT model. The same graph can thus be used as the basis for developing simplified models, without explicitly modelling SSPT, but informing the model of the microconstituents that are expected to be present.

The model that was used was validated against a series of experimental data. The data that are extensively presented here are three independent sets of residual stress measurements; one set of contour method data (performed at The University of Manchester) and two sets of neutron diffraction measurements (one at Engin-X, UK and the second one at Kowari, Australia).

Acknowledgements

This research forms part of the EPSRC funded New Nuclear MANufacturing (NNUMAN) Program (EP/J021172/1). Professor M.C. Smith is partly supported through the EPSRC Fellowship in Manufacturing (EP/L015013/1).

The authors would like to thank the Manufacturing Technology Research Laboratory (MTRL) staff, Ian Winstanley and Paul English; the NNUMAN Programme manager Dr Neil Irvine and the NNUMAN project manager Jacqui Grant, Dr Ondrej Muránsky and Prof Anna Paradowska from ANSTO; Dr Saurabh Kabra at Engin-X, Dr Arben Ferhati, Mike Nunn and Kyle Power, TWI, Cambridge, UK for the manufacturing of the RPEB welds. The authors gratefully acknowledge the award of the RB1410434 and RB1320295 neutron beam times at Engin-X, Oxford, UK and the beam time at Kowari, ANSTO, AU.

References

[1] J.A. Francis, H.K.D.H. Bhadeshia, P.J. Withers, Mater. Sci. Technol. 23 (2007) 1009–1020.
[2] K.R. Ayres, P.R. Hurrell, C.M. Gill, K. Bridger, L.D. Burling, C.S. Punshon, L. Wei, N. Bagshaw, in: Proc. ASME 2010 Press. Vessel. &Piping Conf. PVP2010-25957, 2010.
[3] Y. Javadi, M.C. Smith, K. Abburi Venkata, N. Naveed, A.N. Forsey, J.A. Francis, R.A. Ainsworth, C.E. Truman, D.J. Smith, F. Hosseinzadeh, S. Gungor, P.J. Bouchard, H.C. Dey, A.K. Bhaduri, S. Mahadevan, Int. J. Press. Vessel. Pip. 154 (2017) 41–57.
[4] A. Kundu, P.J. Bouchard, S. Kumar, K. a Venkata, J.A. Francis, A. Paradowska, G.K. Dey, C.E. Truman, Sci. Technol. Weld. Join. 18 (2013) 70–75.
[5] P.R. Hurrell, B.M.E. Pellereau, C.M. Gill, E. Kingston, D. Smith, P.J. Bouchard, in: Proc. ASME 2014 Press. Vessel. Pip. Conf. PVP2014-28809, 2014.
[6] J. Balakrishnan, A.N. Vasileiou, J.A. Francis, M.C. Smith, M.J. Roy, M.D. Callaghan, N.M. Irvine, Int. J. Press. Vessel. Pip. (2018).
[7] D.W. Rathod, J.A. Francis, A.N. Vasileiou, M.J. Roy, P.D. English, J. Balakrishnan, M.C. Smith, N.M. Irvine, Int. J. Press. Vessel. Pip. 172 (2019) 313–328.
[8] A.N. Vasileiou, M.C. Smith, J.A. Francis, D.W. Rathod, J. Balakrishnan, N.M. Irvine, Int. J. Press. Vessel. Pip. 172 (2019) 379–390.
[9] B.G. Zhang, G.Q. Chen, W. Guo, M.X. Shi, Appl. Mech. Mater. 152–154 (2012) 665–671.
[10] K.A. Venkata, C.E. Truman, in: Proc. ASME 2013 Press. Vessel. Pip. Conf. PVP2013, Paris, France, 2013.
[11] O. Muránsky, C.J. Hamelin, M.C. Smith, P.J. Bendeich, L. Edwards, Comput. Mater. Sci. 54 (2012) 125–134.
[12] I. Sattari-Far, Y. Javadi, Int. J. Press. Vessel. Pip. 85 (2008) 265–274.
[13] C.J. Hamelin, O. Muránsky, M.C. Smith, T.M. Holden, V. Luzin, P.J. Bendeich, L. Edwards, Acta Mater. 75 (2014) 1–19.
[14] Vasileiou A.N., Smith M.C., Jeyaganesh B., Francis J., Hamelin C., Nucl. Eng. Des. (2017) 309–316.
[15] C.J. Hamelin, O. Muránsky, V. Luzin, P. Bendeich, L. Edwards, in: ASME (Ed.), Proc. ASME 2011 Press. Vessel. Pip. Div. PVP2011-57426, Baltimore, Maryland, USA, 2011, pp. 1–9.
[16] N. O'Meara, H. Abdolvand, J.A. Francis, S.D. Smith, P.J. Withers, Mater. Sci. Technol. 0836 (2016) 160128015948009.
[17] V.I. Patel, O. Muránsky, C.J. Hamelin, M.D. Olson, M.R. Hill, L. Edwards, Mater. Sci. Forum 777 (2014) 46–51.
[18] Y. Sun, C. Hamelin, T.F. Flint, Q. Xiong, A.N. Vasileiou, I. Pantelis, J.A. Francis, M.C. Smith, Math. Model. Weld Phenom. 12 (2019) 149–165.
[19] Y.L. Sun, G. Obasi, C.J. Hamelin, A.N. Vasileiou, T.F. Flint, J. Balakrishnan, M.C. Smith, J.A. Francis, J. Mater. Process. Technol. 265 (2019) 71–86.
[20] N.O. Meara, S.D. Smith, J.A. Francis, in: Proc. ASME 2015 Press. Vessel. Pip. Conf. PVP2015-45936, 2016.
[21] H. Pous-Romero, I. Lonardelli, D. Cogswell, H.K.D.H. Bhadeshia, Mater. Sci. Eng. A 567 (2013) 72–79.
[22] G. Obasi, E.J. Pickering, A.N. Vasileiou, Y.L. Sun, D. Rathod, M. Preuss, J.A. Francis, M.C. Smith, Metall. Mater. Trans. A Phys. Metall. Mater. Sci. 50 (2019) 1715–1731.
[23] J. Balakrishnan, A.N. Vasileiou, J.A. Francis, M.C. Smith, M.J. Roy, M.D. Callaghan, N.M. Irvine, Int. J. Press. Vessel. Pip. (2018).
[24] B. Jeyaganesh, M.D. Callaghan, J.A. Francis, P.D. English, A.N. Vasileiou, M.J. Roy, W. Guo, N.M. Irvine, M.C. Smith, L. Li, A.H. Sherry, in: ASME (Ed.), Proc. ASME 2014 Press. Vessel. Pip. Conf. PVP2014, California, USA, 2014.
[25] A.N. Vasileiou, M.C. Smith, D. Gandy, A. Ferhati, R. Romac, S. Paddea, in: Proc. ASME 2016 Press. Vessel. Pip. Conf. PVP2016, American Society of Mechanical Engineers(ASME), Vancouver, British Columbia, Canada, 2016, pp. 1–11.
[26] H.K.D.H. Bhadeshia, Mater. Sci. Technol. (United Kingdom) 8 (1992) 123–133.
[27] R.M. Smith, FEAT-WMT : Weld-Modelling Tool User Guide, FeatPlus Limited, Bristol, Uk, 2013.
[28] Flint, J.A. Francis, M.. Smith, Vasileiou A.N., Int. J. Press. Vessel. Pip. 123 (2018) 140–150.
[29] L.E. Pol, G. Weng, Int. J. Plast. 5 (1989) 573–591.
[30] M.V. Li, D. V Niebuhr, L.L. Meekisho, D.G. Atteridge, Metall. Mater. Trans. B 29 (1998) 661–672.
[31] M.C. Smith, A.C. Smith, C. Ohms, R.C. Wimpory, Int. J. Press. Vessel. Pip. 164 (2018) 3–21.